



Three New Low-Energy Resonances in the $^{22}\text{Ne}(p,\gamma)^{23}\text{Na}$ Reaction

F. Cavanna,¹ R. Depalo,² M. Aliotta,³ M. Anders,^{4,5} D. Bemmerer,^{4,†} A. Best,⁶ A. Boeltzig,⁷ C. Broggini,⁸ C. G. Bruno,³ A. Cacioli,² P. Corvisiero,¹ T. Davinson,⁹ A. di Leva,¹⁰ Z. Elekes,¹¹ F. Ferraro,¹ A. Formicola,⁶ Zs. Fülöp,¹¹ G. Gervino,¹² A. Guglielmetti,¹³ C. Gustavino,¹⁴ Gy. Gyürky,¹¹ G. Imbriani,¹⁰ M. Junker,⁶ R. Menegazzo,⁸ V. Mossa,¹⁵ F. R. Pantaleo,¹⁵ P. Prati,¹ D. A. Scott,⁹ E. Somorjai,¹¹ O. Straniero,¹⁶ F. Strieder,^{17,*} T. Szücs,⁴ M. P. Takács,^{4,5} and D. Trezzi¹³

(The LUNA Collaboration)

¹Università degli Studi di Genova and INFN, Sezione di Genova, Via Dodecaneso 33, 16146 Genova, Italy

²Università degli Studi di Padova and INFN, Sezione di Padova, Via F. Marzolo 8, 35131 Padova, Italy

³SUPA, School of Physics and Astronomy, University of Edinburgh, EH9 3FD Edinburgh, United Kingdom

⁴Helmholtz-Zentrum Dresden-Rossendorf, Bautzner Landstr. 400, 01328 Dresden, Germany

⁵Technische Universität Dresden, Institut für Kern- und Teilchenphysik, Zellescher Weg 19, 01069 Dresden, Germany

⁶Laboratori Nazionali del Gran Sasso (LNGS), 67100 Assergi (AQ), Italy

⁷Gran Sasso Science Institute, 67100 L'Aquila, Italy

⁸INFN, Sezione di Padova, Via F. Marzolo 8, 35131 Padova, Italy

⁹SUPA, School of Physics and Astronomy, University of Edinburgh, EH9 3JZ Edinburgh, United Kingdom

¹⁰Università di Napoli Federico II and INFN, Sezione di Napoli, 80126 Napoli, Italy

¹¹Institute for Nuclear Research (MTA ATOMKI), PO Box 51, HU-4001 Debrecen, Hungary

¹²Università degli Studi di Torino and INFN, Sezione di Torino, Via P. Giuria 1, 10125 Torino, Italy

¹³Università degli Studi di Milano and INFN, Sezione di Milano, Via G. Celoria 16, 20133 Milano, Italy

¹⁴INFN, Sezione di Roma La Sapienza, Piazzale A. Moro 2, 00185 Roma, Italy

¹⁵Università degli Studi di Bari and INFN, Sezione di Bari, 70125 Bari, Italy

¹⁶Osservatorio Astronomico di Collurania, Teramo, and INFN, Sezione di Napoli, Napoli, Italy

¹⁷Institut für Experimentalphysik III, Ruhr-Universität Bochum, 44780 Bochum, Germany

(Received 17 September 2015; published 15 December 2015)

The $^{22}\text{Ne}(p,\gamma)^{23}\text{Na}$ reaction takes part in the neon-sodium cycle of hydrogen burning. This cycle affects the synthesis of the elements between ^{20}Ne and ^{27}Al in asymptotic giant branch stars and novae. The $^{22}\text{Ne}(p,\gamma)^{23}\text{Na}$ reaction rate is very uncertain because of a large number of unobserved resonances lying in the Gamow window. At proton energies below 400 keV, only upper limits exist in the literature for the resonance strengths. Previous reaction rate evaluations differ by large factors. In the present work, the first direct observations of the $^{22}\text{Ne}(p,\gamma)^{23}\text{Na}$ resonances at 156.2, 189.5, and 259.7 keV are reported. Their resonance strengths are derived with 2%–7% uncertainty. In addition, upper limits for three other resonances are greatly reduced. Data are taken using a windowless ^{22}Ne gas target and high-purity germanium detectors at the Laboratory for Underground Nuclear Astrophysics in the Gran Sasso laboratory of the National Institute for Nuclear Physics, Italy, taking advantage of the ultralow background observed deep underground. The new reaction rate is a factor of 20 higher than the recent evaluation at a temperature of 0.1 GK, relevant to nucleosynthesis in asymptotic giant branch stars.

DOI: 10.1103/PhysRevLett.115.252501

PACS numbers: 25.40.Lw, 26.20.Cd, 26.35.+c

Recent studies of globular clusters with high-resolution spectrometers [1–3] have opened new windows on Galactic chemical evolution. It was found that globular clusters are made up of multiple generations of stars [4,5]. A peculiar observation in this framework is the anticorrelation between oxygen and sodium abundances found in giant stars belonging to all globular clusters studied so far [6–8]. The stellar sources responsible for these effects have not yet been identified. One possible source is massive asymptotic giant branch (AGB) stars (AGB stars with mass $M > 4 M_{\odot}$) where the so-called hot bottom burning (HBB) process is active [6,9,10]. (M_{\odot} is the mass of

our Sun.) Other possibilities include massive binaries [11], fast rotating massive stars [12], and supermassive ($M \sim 10^4 M_{\odot}$) stars [13].

The neon-sodium (NeNa) and magnesium-aluminum (MgAl) cycles of hydrogen burning are activated when the temperature in the hydrogen burning region exceeds ~ 0.07 GK (corresponding to a Gamow energy of $E_p > 100$ keV). (E_p denotes the proton beam energy in the laboratory system.) In the HBB process, the temperature at the base of the convective envelope rises as high as 0.1 GK ($E_p \sim 120$ keV). The NeNa and MgAl chains increase the surface sodium and aluminum abundances and

decrease the magnesium abundance [14]. In parallel, oxygen is depleted by the oxygen-nitrogen (ON) cycle. The interpretation of the observed abundance patterns thus requires a precise knowledge of nucleosynthesis in the NeNa and MgAl chains and in the ON cycle. The MgAl chain [15] and ON cycle [16] have recently been addressed in low-energy experiments. The present work reports on a high-luminosity experiment on the most uncertain reaction of the NeNa cycle, $^{22}\text{Ne}(p, \gamma)^{23}\text{Na}$.

In addition to the AGB star scenario and the HBB process, hydrogen burning of ^{22}Ne also plays a role in explosive nucleosynthesis scenarios. In classical novae ($0.15 < T < 0.45$ GK, $150 < E_p < 300$ keV [20]), the ejected material carries the products of the hot CNO cycle and of the NeNa [21] and MgAl chains. For an oxygen-neon nova, the uncertainty on the $^{22}\text{Ne}(p, \gamma)^{23}\text{Na}$ reaction rate leads to 6 orders of magnitude uncertainty on the ^{22}Ne yield [22]. For a carbon-oxygen nova, $^{22}\text{Ne}(p, \gamma)^{23}\text{Na}$ was found to affect the abundances of elements between neon and aluminum [22]. As a consequence, there is a call for a more precise $^{22}\text{Ne}(p, \gamma)^{23}\text{Na}$ thermonuclear reaction rate [23]. In type Ia supernovae, during preexplosion hydrogen burning ($T < 0.6$ GK, $E_p < 400$ keV) on the surface of the white dwarf star, the $^{22}\text{Ne}(p, \gamma)^{23}\text{Na}$ reaction may deplete ^{22}Ne , hence changing the electron fraction and all the subsequent nucleosynthesis [24]. In core collapse supernova precursors, proton capture on ^{22}Ne competes with the neutron source reaction $^{22}\text{Ne}(\alpha, n)^{25}\text{Mg}$, thus affecting neutron capture nucleosynthesis [25]. Summarizing, new $^{22}\text{Ne}(p, \gamma)^{23}\text{Na}$ data are needed for several highly topical astrophysical scenarios ranging from AGB stars to supernovae.

$^{22}\text{Ne}(p, \gamma)^{23}\text{Na}$ resonances with resonance energy $E_p^{\text{res}} > 400$ keV affect the thermonuclear reaction rate for high temperatures $T > 0.5$ GK, see Ref. [26] for recent new data. For lower temperatures $T < 0.5$ GK relevant to most of the scenarios discussed above [6,9,10,14,20,22–25], the strengths of resonances with $E_p^{\text{res}} < 400$ keV must be known. Only one direct experiment is reported in the literature [27], and it shows only upper limits for the resonance strengths. Indirect data are also available [28–30], but their interpretation relies on spin parity assignments or spectroscopic factor normalizations, which are often uncertain. As a result, the mere existence of the resonances at $E_p^{\text{res}} = 71, 105,$ and 215 keV is still under debate [28,29].

In 1999, NACRE Collaboration [31] derived the $^{22}\text{Ne}(p, \gamma)^{23}\text{Na}$ reaction rate from resonance strengths [27,32,33] and a small direct capture component [32]. A similar evaluation was performed by Hale *et al.* in 2001 [29], updated by Iliadis *et al.* in 2010 [34,35] and again in 2013 by the STARLIB group [36], including new indirect data [29]. Iliadis *et al.* used much lower upper limits than NACRE Collaboration in several cases and excluded some

debated resonances from consideration [34–36]. As a result, there is up to a factor of 1000 difference in the total reaction rate between NACRE Collaboration and the STARLIB group [31,36]. The aim of the present work is to address this unsatisfactory situation with high-statistics, direct experimental data.

The measurements were carried out at the Laboratory for Underground Nuclear Astrophysics (LUNA) in the underground facility of the Italian National Institute for Nuclear Physics Gran Sasso National Laboratory, which offers an unprecedented sensitivity thanks to its low-background environment [37,38]. Several nuclear reactions of astrophysical importance have been studied at very low energies at LUNA in recent years [16,39,40]. The experimental setup (Refs. [17–19] and Fig. 1) consists of a windowless gas target chamber filled with 1.5 mbar ^{22}Ne gas (isotopic enrichment 99.9%, recirculated through a Monotorr II PS4-MT3-R-2 chemical getter) and two large high-purity germanium detectors, respectively, at a 55° (Ge55) and at a 90° angle (Ge90) to the beam axis. Possible gas impurities by in-leaking air were periodically checked by the strong $E_p^{\text{res}} = 278$ keV $^{14}\text{N}(p, \gamma)^{15}\text{O}$ resonance and were always below 0.1%.

The 70–300 keV proton beam from the LUNA 400 kV accelerator [41] (beam current 100–250 μA) is collimated through a series of long, narrow apertures, then enters the target chamber, and is finally stopped on a copper beam calorimeter with a constant temperature gradient. Ge90 and Ge55 are surrounded by a 4π lead shield of 22–30 cm thickness, and a 4 cm inner copper liner for Ge55. The γ -ray detection efficiency was measured ($478 \leq E_\gamma \leq 1836$ keV) with calibrated radioactive sources (^7Be , ^{60}Co , ^{88}Y , ^{137}Cs)

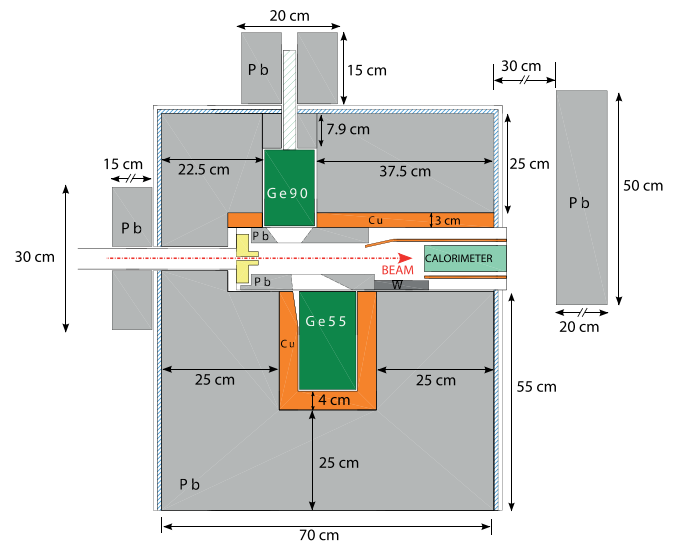


FIG. 1 (color online). Target chamber, germanium detectors (Ge55 and Ge90), and copper (orange) and lead (gray) shielding. The external lead wall on the right-hand side covers the shielding gap where the calorimeter is inserted [17–19].

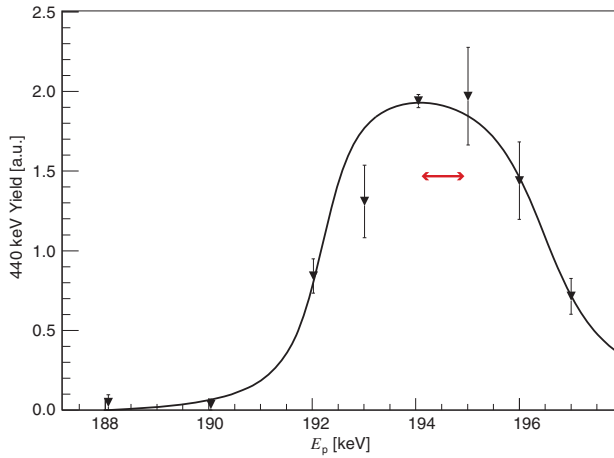


FIG. 2 (color online). Ge55 scan of the resonance at $E_p^{\text{res}} = 189.5$ keV. The maximum at $E_p = 194.5$ keV corresponds to a resonance energy of (189.5 ± 0.7) keV. The red arrow indicates the uncertainty on the resonance energy. The black line is just to guide the eye.

and extended to higher energies ($765 \leq E_\gamma \leq 6790$ keV) by the isotropic 1:1 photon cascades of the $^{14}\text{N}(p, \gamma)^{15}\text{O}$ resonance at $E_p^{\text{res}} = 278$ keV.

As a first step, the energies of the resonances at $E_p^{\text{res}} = 271.6$ keV in the $^{21}\text{Ne}(p, \gamma)^{22}\text{Na}$ and 384.5 keV in the $^{20}\text{Ne}(p, \gamma)^{21}\text{Na}$ reactions have been remeasured, relative to the accelerator energy calibration ($\Delta E_p = 0.3$ keV [41]). Using neon gas of natural isotopic composition (90.48% ^{20}Ne , 0.27% ^{21}Ne , 9.25% ^{22}Ne), resonance energies of 271.5 ± 1.0 and 385.6 ± 0.6 keV, respectively, were found, consistent with the literature [35,42]. This confirms

that the accelerator energy calibration and energy loss in the gas are properly understood.

Each of the suspected $^{22}\text{Ne}(p, \gamma)^{23}\text{Na}$ resonances [27,35] was first scanned with 3–9 beam energy steps of 1–2 keV (Fig. 2). If a resonance was indeed detected, its energy was then obtained by matching the yield profile for the 440 keV γ ray (deexcitation of the first excited state in ^{23}Na) with the efficiency profile taken with the ^7Be source ($E_\gamma = 478$ keV). New $^{22}\text{Ne}(p, \gamma)^{23}\text{Na}$ resonances were found at 156.2 ± 0.7 , 189.5 ± 0.7 , and 259.7 ± 0.6 keV. The uncertainty includes a 1.7% error on the proton energy loss in neon gas (~ 0.5 keV/cm) [43]. The corresponding ^{23}Na excitation energies are consistent with, but more precise than, the literature values [30,35] except for the resonance at 189.5 keV. The reported [30] and adopted [35] level energy of $E_x = 8972$ keV is instead found to be 8975.3 ± 0.7 keV here. After the scan, high-statistics runs (typical running time 58 h on top of the $E_p^{\text{res}} = 156.2$ keV resonance) were performed at the maximum of the yield profile and, to determine the nonresonant yield, well outside the resonance profile (Fig. 2) at 9–53 keV distance in an area without other suspected resonances and with a low beam-induced background. The observed on-resonance spectra are dominated by the resonance under study, see Fig. 3 for typical Ge55 spectra. The nonresonant yield was always found to be consistent with zero for the resonances observed here.

The resonance strength $\omega\gamma$ was then determined from the total yield Y_{max} given by the sum of the primary transitions, (i.e., transitions from the resonance under study to a given state in ^{23}Na) after correcting for detection efficiency:

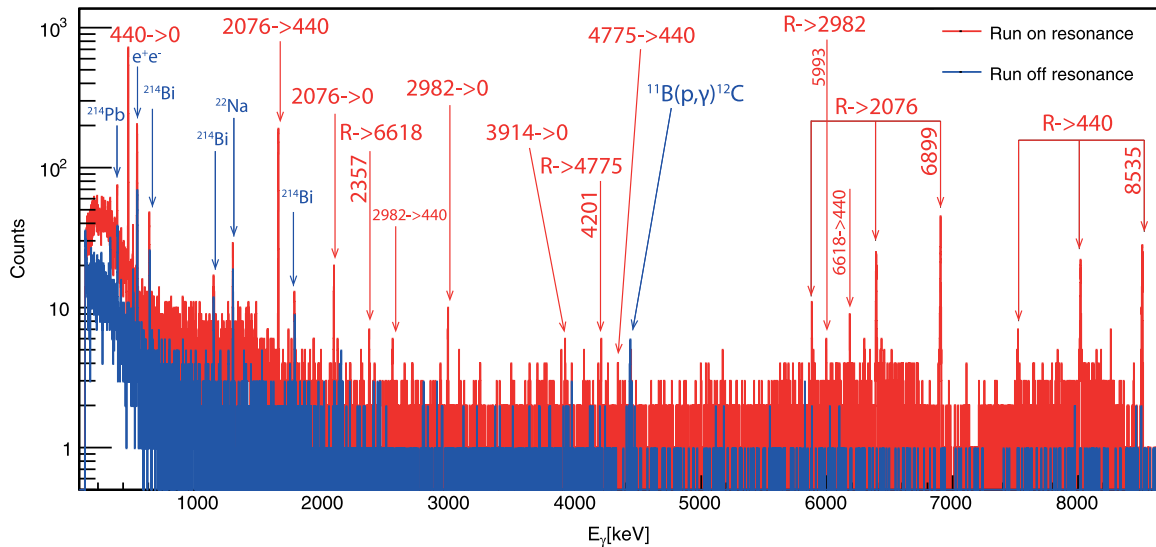


FIG. 3 (color online). Spectra taken with Ge55 at $E_p = 195$ keV, on the top of the 189.5 keV resonance (red), and at $E_p = 221$ keV, well outside the resonance profile, scaled by a factor of 0.99 for equal charge (blue). Red arrows show $^{22}\text{Ne}(p, \gamma)^{23}\text{Na}$ transitions (“R” denotes the resonance; numbers denote the ^{23}Na excitation energy in keV). Blue arrows show background lines.

$$\omega\gamma = \frac{2Y_{\max}\epsilon_R}{\lambda_R^2} \frac{m_t}{m_t + m_p}, \quad (1)$$

where ϵ_R is the effective stopping power in the laboratory system, λ_R^2 is the squared de Broglie wavelength at the resonance energy, and m_t and m_p are the masses of the target and projectile, respectively. The spin-parity of the resonances shown here is partly still under study [30]; therefore, theoretical predictions of the angular distributions are fraught with uncertainty. For each resonance, the $\omega\gamma$ data obtained by separately analyzing Ge55 and Ge90 were found to be mutually consistent within 3%–14% statistical uncertainty. Isotropy was then assumed, and the weighted average of Ge55 and Ge90 was adopted (Table I). The systematic uncertainty includes 3% uncertainty on the γ detection efficiency, 1.1% on the effective gas density [17], and 1% on the beam current.

Sources of beam induced background include the $^{11}\text{B}(p,\gamma)^{12}\text{C}$, $^{12}\text{C}(p,\gamma)^{13}\text{N}$, and $^{19}\text{F}(p,\alpha\gamma)^{16}\text{O}$ reactions [17]. The former two have only negligible impact. The latter affects spectra for $E_p > 340$ keV [17]. Even given this background, for example, in Fig. 3 the continuum at 6–8 MeV is still a factor of 50 lower than the no-beam background at the surface of the Earth [44].

The present resonance strength values are consistent with the previous direct upper limits [27], with the exception of the resonance at $E_p^{\text{res}} = 259.7$ keV, which is slightly stronger than the previous upper limit (Table I). Interesting discrepancies appear when comparing the present direct data with the previous indirect upper limits. For the resonances at 156.2 and 259.7 keV, the present strengths are a factor of 16 and 50, respectively, higher than the indirect upper limits [29,35]. For these two states, only limited angular distribution data were available in the indirect works [29], hampering their interpretation. Indeed, new spin-parity values reported recently [30] are somewhat different from those in Ref. [29]. Together with possible normalization issues, this fact might explain the

discrepancy with the present direct data. In the present measurement there was no evidence of the suspected weak resonances at 71, 105, and 215 keV. The profile likelihood method [45] has been used to derive new upper limits (90% confidence level) from the present data for these cases. The new upper limits (Table I) are much improved with respect to the literature. Resonances at $E_p^{\text{res}} = 290$ –400 keV were not explored here, because the previous direct [27] and indirect [29] upper limits already show that they contribute only negligibly, $< 1\%$, to the total thermonuclear reaction rate.

Using the present new low-energy resonance strengths at novae and AGB star energies (Table I), literature strengths [26,35] at energies not explored here, and the previously assumed nonresonant S factor of 62 keVb [35] (contributing $< 5\%$ to the rate), the thermonuclear reaction rate was calculated in the temperature range 0.02–1GK. The resonant contribution, in units of $\text{cm}^3 \text{mol}^{-1} \text{s}^{-1}$, is given by [31]

$$N_A \langle \sigma v \rangle_R = \frac{1.5394 \times 10^5}{(\mu T_9)^{3/2}} \sum_i (\omega\gamma)_i e^{-11.605 E_i^{\text{res}}/T_9}, \quad (2)$$

where N_A denotes Avogadro's constant, T_9 is the temperature in units of GK, $\omega\gamma_i$ is the resonance strength in eV (Table I, last column), and μ and E_i^{res} are the reduced mass (in amu) and the resonance energy in the center of mass (in MeV). In order to estimate the total rate and its uncertainty, a Monte Carlo method has been employed: (i) for each resonance, the two input parameters resonance energy and strength are each sampled from a Gaussian probability density distribution, taking into account their values and uncertainties, from the present data, where available, and from the literature [34] for the other cases; (ii) the reaction rate is calculated for a set of temperatures in the 0.02–1GK range; (iii) steps (i)–(ii) are repeated 10 000 times. For the resonances at 71, 105, and 215 keV, where only upper

TABLE I. $^{22}\text{Ne}(p,\gamma)^{23}\text{Na}$ resonance strengths from the literature and from the present work. The error bar on the strength measured in this work includes both statistical and systematic uncertainties.

| Energy [keV] | | Strength $\omega\gamma$ [eV] | | | | | |
|--------------------|------------------|------------------------------|-------------------------------|--------------------------|------------------------------------|---------------------------|---------------------------|
| E_p^{res} | E_x | Previous direct | Previous indirect | NACRE [31] adopted | Iliadis <i>et al.</i> [35] adopted | Present work direct | Present work adopted |
| 29 | 8822 | ... | $\leq 2.610^{-25}$ [35] | ... | $\leq 2.610^{-25}$ | ... | $\leq 2.610^{-25}$ |
| 37 | 8829 | ... | $(3.1 \pm 1.2) 10^{-15}$ [35] | $(6.8 \pm 1.0) 10^{-15}$ | $(3.1 \pm 1.2) 10^{-15}$ | ... | $(3.1 \pm 1.2) 10^{-15}$ |
| 71 | 8862 | $\leq 3.210^{-6}$ [27] | $\leq 1.910^{-10}$ [29] | $\leq 4.210^{-9}$ | ... | $\leq 1.510^{-9}$ | $\leq 1.510^{-9}$ |
| 105 | 8895 | $\leq 0.610^{-6}$ [27] | $\leq 1.410^{-7}$ [29] | $\leq 6.010^{-7}$ | ... | $\leq 7.610^{-9}$ | $\leq 7.610^{-9}$ |
| 156.2 ± 0.7 | 8943.5 ± 0.7 | $\leq 1.010^{-6}$ [27] | $(9.2 \pm 3.7) 10^{-9}$ [35] | $(6.5 \pm 1.9) 10^{-7}$ | $(9.2 \pm 3.7) 10^{-9}$ | $[1.48 \pm 0.10] 10^{-7}$ | $[1.48 \pm 0.10] 10^{-7}$ |
| 189.5 ± 0.7 | 8975.3 ± 0.7 | $\leq 2.610^{-6}$ [27] | $\leq 2.610^{-6}$ [29] | $\leq 2.610^{-6}$ | $\leq 2.610^{-6}$ | $[1.87 \pm 0.06] 10^{-6}$ | $[1.87 \pm 0.06] 10^{-6}$ |
| 215 | 9000 | $\leq 1.410^{-6}$ [27] | ... | $\leq 1.410^{-6}$ | ... | $\leq 2.810^{-8}$ | $\leq 2.810^{-8}$ |
| 259.7 ± 0.6 | 9042.4 ± 0.6 | $\leq 2.610^{-6}$ [27] | $\leq 1.310^{-7}$ [29] | $\leq 2.610^{-6}$ | $\leq 1.310^{-7}$ | $[6.89 \pm 0.16] 10^{-6}$ | $[6.89 \pm 0.16] 10^{-6}$ |
| 291 | 9072 | $\leq 2.210^{-6}$ [27] | ... | $\leq 2.210^{-6}$ | $\leq 2.210^{-6}$ | ... | $\leq 2.210^{-6}$ |
| 323 | 9103 | $\leq 2.210^{-6}$ [27] | ... | $\leq 2.210^{-6}$ | $\leq 2.210^{-6}$ | ... | $\leq 2.210^{-6}$ |
| 334 | 9113 | $\leq 3.010^{-6}$ [27] | ... | $\leq 3.010^{-6}$ | $\leq 3.010^{-6}$ | ... | $\leq 3.010^{-6}$ |
| 369 | 9147 | ... | $\leq 6.010^{-4}$ [29] | ... | $\leq 6.010^{-4}$ | ... | $\leq 6.010^{-4}$ |
| 394 | 9171 | ... | $\leq 6.010^{-4}$ [29] | ... | $\leq 6.010^{-4}$ | ... | $\leq 6.010^{-4}$ |

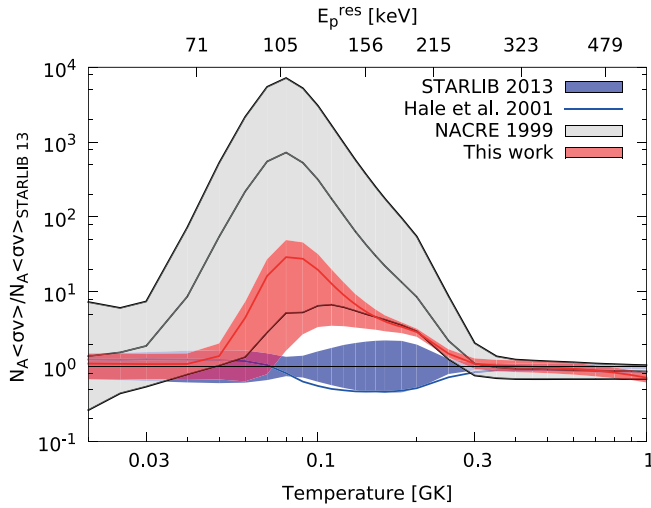


FIG. 4 (color online). Thermonuclear reaction rate of this work, NACRE Collaboration [31], Hale *et al.* [29], and the STARLIB group [36] normalized to the STARLIB group [36].

limits exist, in step (ii) the resonance strength was sampled by separately sampling Poisson distributions for the signal and background excluding unphysical negative values when taking the difference [45]. This procedure yields the probability density function and thus a median value and uncertainty of the reaction rate at each temperature. In order to be very conservative, for the lower side of the 1σ error band the unobserved resonances at 71, 105, and 215 keV were forced to zero, exactly as the STARLIB group [34–36] did for these resonances.

The central value of the present new thermonuclear reaction rate lies between those of NACRE Collaboration and the STARLIB group [36] (Fig. 4). It is consistent, within the previous significant error bars, with NACRE Collaboration. The new 1σ lower limit is above the previous upper limit by the STARLIB group [36] for $0.08 < T < 0.25$ GK, mainly because of the newly observed resonances at 156.2, 189.5, and 259.7 keV. The larger error bar at low temperatures, 0.05–0.1 GK, is explained by the different treatment of the 71, 105, and 215 keV resonances. In the present work, they are set to zero for the lower error bar, but the Monte Carlo approach includes them for the median value and upper error bar. Previously, they were excluded and did not contribute to the uncertainty [34–36].

In order to illustrate the impact of the new rate on ^{23}Na and the Na-O anticorrelation, previous calculated ^{23}Na yields for intermediate mass AGB stars [46] are used here. That calculation [46] used the Hale *et al.* [29] reaction rate as the control value; the present rate is a factor of 10–30 higher at HBB temperatures. The new rate leads to an enhancement of the predicted ^{23}Na yield by a factor of 3 for an AGB star model of $5 M_{\odot}$ and initial metallicity $Z = 0.008$ [46]. Other HBB simulations [10] have reported

that the most oxygen-poor ejecta are also sodium rich, again based on the Hale *et al.* [29] rate. These ejecta [10] will become even more sodium rich, by about a factor of 3, based on the present, new rate.

Summarizing, the $^{22}\text{Ne}(p,\gamma)^{23}\text{Na}$ reaction has been studied by underground in-beam γ spectroscopy using a windowless gas target. Three low-energy resonances have been observed for the first time, leading to a significant increase of the thermonuclear reaction rate at temperatures $0.08 \leq T \leq 0.3$ GK relevant to AGB stars, hot bottom burning, and novae. Significantly reduced upper limits were obtained for three more resonances; for further progress here, a new experiment with even higher luminosity is needed.

Financial support by INFN, DFG (Grant No. BE 4100-2/1), NAVI (Grant No. HGF VH-VI-417), and OTKA (Grant No. K101328), and the support of a DAAD fellowship at HZDR for F. C. are gratefully acknowledged.

*Present address: South Dakota School of Mines and Technology, Rapid City, South Dakota 57701, USA.

†d.bemmerer@hzdr.de

- [1] E. Carretta, S. Lucatello, R. G. Gratton, A. Bragaglia, and V. D’Orazi, *Astron. Astrophys.* **533**, A69 (2011).
- [2] K. Lind, C. Charbonnel, T. Decressin, F. Primas, F. Grundahl, and M. Asplund, *Astron. Astrophys.* **527**, A148 (2011).
- [3] D. Yong, F. Grundahl, D. L. Lambert, P. E. Nissen, and M. D. Shetrone, *Astron. Astrophys.* **402**, 985 (2003).
- [4] R. G. Gratton, E. Carretta, and A. Bragaglia, *Astron. Astrophys. Rev.* **20**, 50 (2012).
- [5] M. J. Cordero, C. A. Pilachowski, C. I. Johnson, and E. Vesperini, *Astrophys. J.* **800**, 3 (2015).
- [6] R. Gratton, C. Sneden, and E. Carretta, *Annu. Rev. Astron. Astrophys.* **42**, 385 (2004).
- [7] E. Carretta *et al.*, *Astron. Astrophys.* **505**, 117 (2009).
- [8] C. I. Johnson and C. A. Pilachowski, *Astrophys. J. Lett.* **754**, L38 (2012).
- [9] A. Renzini and M. Voli, *Astron. Astrophys.* **94**, 175 (1981).
- [10] P. Ventura and F. D’Antona, *Astron. Astrophys.* **479**, 805 (2008).
- [11] S. E. de Mink, O. R. Pols, N. Langer, and R. G. Izzard, *Astron. Astrophys.* **507**, L1 (2009).
- [12] T. Decressin, G. Meynet, C. Charbonnel, N. Prantzos, and S. Ekström, *Astron. Astrophys.* **464**, 1029 (2007).
- [13] P. A. Denissenkov and F. D. A. Hartwick, *Mon. Not. R. Astron. Soc.* **437**, L21 (2014).
- [14] P. A. Denissenkov and S. N. Denisenkova, *Sov. Astron. Lett.* **16**, 275 (1990).
- [15] F. Strieder *et al.*, *Phys. Lett. B* **707**, 60 (2012).
- [16] D. A. Scott *et al.*, *Phys. Rev. Lett.* **109**, 202501 (2012).
- [17] F. Cavanna *et al.*, *Eur. Phys. J. A* **50**, 179 (2014).
- [18] R. Depalo, PhD thesis, Università di Padova, 2015.
- [19] F. Cavanna, PhD thesis, Università di Genova, 2015.
- [20] J. José and M. Hernanz, *Astrophys. J.* **494**, 680 (1998).
- [21] A. L. Sallaska, C. Wrede, A. Garcia, D. W. Storm, T. A. D. Brown, C. Ruiz, K. A. Snover, D. F. Ottewell, L. Buchmann,

- C. Vockenhuber, D. A. Hutcheon, and J. A. Caggiano, *Phys. Rev. Lett.* **105**, 152501 (2010).
- [22] C. Iliadis, A. Champagne, J. José, S. Starrfield, and P. Tupper, *Astrophys. J. Suppl. Ser.* **142**, 105 (2002).
- [23] P. A. Denissenkov, J. W. Truran, M. Pignatari, R. Trappitsch, C. Ritter, F. Herwig, U. Battino, K. Setoodehnia, and B. Paxton, *Mon. Not. R. Astron. Soc.* **442**, 2058 (2014).
- [24] D. A. Chamulak, E. F. Brown, F. X. Timmes, and K. Dupczak, *Astrophys. J.* **677**, 160 (2008).
- [25] M. Pignatari, E. Zinner, P. Hoppe, C. J. Jordan, B. K. Gibson, R. Trappitsch, F. Herwig, C. Fryer, R. Hirschi, and F. X. Timmes, *Astrophys. J. Lett.* **808**, L43 (2015).
- [26] R. Depalo, F. Cavanna, F. Ferraro, A. Slemer, T. Al-Abdullah, S. Akhmadaliev, M. Anders, D. Bemmerer, Z. Elekes, G. Mattei, S. Reinicke, K. Schmidt, C. Scian, and L. Wagner, *Phys. Rev. C* **92**, 045807 (2015).
- [27] J. Görres, C. Rolfs, P. Schmalbrock, H. P. Trautvetter, and J. Keinonen, *Nucl. Phys.* **385A**, 57 (1982).
- [28] J. R. Powers, H. T. Fortune, R. Middleton, and O. Hansen, *Phys. Rev. C* **4**, 2030 (1971).
- [29] S. E. Hale, A. E. Champagne, C. Iliadis, V. Y. Hansper, D. C. Powell, and J. C. Blackmon, *Phys. Rev. C* **65**, 015801 (2001).
- [30] D. G. Jenkins, M. Bouhelal, S. Courtin, M. Freer, B. R. Fulton, F. Haas, R. V. F. Janssens, T. L. Khoo, C. J. Lister, E. F. Moore, W. A. Richter, B. Truett, and A. H. Wuosmaa, *Phys. Rev. C* **87**, 064301 (2013).
- [31] C. Angulo *et al.*, *Nucl. Phys.* **656A**, 3 (1999).
- [32] J. Görres, H. W. Becker, L. Buchmann, C. Rolfs, P. Schmalbrock, H. P. Trautvetter, A. Vlieks, J. W. Hammer, and T. R. Donoghue, *Nucl. Phys.* **408A**, 372 (1983).
- [33] M. Meyer and J. Smit, *Nucl. Phys.* **205A**, 177 (1973).
- [34] C. Iliadis, R. Longland, A. E. Champagne, A. Coc, and R. Fitzgerald, *Nucl. Phys.* **841A**, 31 (2010).
- [35] C. Iliadis, R. Longland, A. E. Champagne, and A. Coc, *Nucl. Phys.* **841A**, 251 (2010).
- [36] A. L. Sallaska, C. Iliadis, A. E. Champagne, S. Goriely, S. Starrfield, and F. X. Timmes, *Astrophys. J. Suppl. Ser.* **207**, 18 (2013).
- [37] H. Costantini, A. Formicola, G. Imbriani, M. Junker, C. Rolfs, and F. Strieder, *Rep. Prog. Phys.* **72**, 086301 (2009).
- [38] C. Broggini, D. Bemmerer, A. Guglielmetti, and R. Menegazzo, *Annu. Rev. Nucl. Part. Sci.* **60**, 53 (2010).
- [39] D. Bemmerer *et al.*, *Phys. Rev. Lett.* **97**, 122502 (2006).
- [40] M. Anders *et al.*, *Phys. Rev. Lett.* **113**, 042501 (2014).
- [41] A. Formicola *et al.*, *Nucl. Instrum. Methods Phys. Res., Sect. A* **507**, 609 (2003).
- [42] H. W. Becker, H. Ebbing, W. H. Schulte, S. Wüstenbecker, M. Berheide, M. Buschmann, C. Rolfs, G. E. Mitchell, and J. S. Schweitzer, *Z. Phys. A* **343**, 361 (1992).
- [43] J. F. Ziegler, M. D. Ziegler, and J. P. Biersack, *Nucl. Instrum. Methods Phys. Res., Sect. B* **268**, 1818 (2010).
- [44] T. Szücs *et al.*, *Eur. Phys. J. A* **44**, 513 (2010).
- [45] W. A. Rolke and A. M. López, *Nucl. Instrum. Methods Phys. Res., Sect. A* **458**, 745 (2001).
- [46] R. G. Izzard, M. Lugaro, A. I. Karakas, C. Iliadis, and M. van Raai, *Astron. Astrophys.* **466**, 641 (2007).